Comprehensive Multiphysics Analysis of High-Energy Nanosecond Lasers Based on Liquid-Cooled Nd-Doped Rods Pumped by Flashlamps

Jianyu Sun (孙剑宇) [1, 2], Yujie Peng (彭宇杰)[1, 2, *], Yingbin Long (龙应斌)[1], Junchi Chen (陈俊驰)[1], Zebiao Gan (甘泽彪)[1], Bo Yao (姚波)[1], Xiaoyan Liang (梁晓燕)[1], Yuxin Leng (冷雨欣)[1, 2, **], and Ruxin Li (李儒新)[1, *]**

1State Key Laboratory of High Field Laser Physics and CAS Center for Excellence in Ultra-intense Laser Science, Shanghai Institute of Optics and Fine Mechanics (SIOM), Chinese Academy of Sciences (CAS), Shanghai 201800, China

2Center of Materials Science and Optoelectronics Engineering, University of Chinese Academy of Sciences, Beijing 100049, China

**Corresponding author: yjpeng@siom.ac.cn; ** corresponding author: lengyuxin@mail.siom.ac.cn;*

**** corresponding author: ruxinli@mail.shcnc.ac.cn*

Ultra-short pulse, ultra-intense (USUI) lasers have become indispensable tools for scientific research. High-energy pump lasers are crucial to ensure adequate energy and beam quality of these USUI lasers. Pump lasers with rod amplifiers are a cost-effective and reliable option for meeting the high-energy pump requirements. However, there is a notable dearth of comprehensive reports on the design of high-energy rod amplifiers. This study provides a detailed analysis of rod amplifiers, focusing primarily on the pump unit utilized at SULF-10PW and SEL-100PW prototype. The analysis covers aspects such as gain management, thermal effects and spatiotemporal evolution.

Keywords: high-energy laser; all-solid-state laser; rod amplifier;
DOI: 10.3788/COLXXXXXX.XXXXXX.

1. Introdction

USUI lasers have opened up new experimental capabilities for High-Energy-Density (HED) Science [1], high harmonic generation (HHG) [2], laser-driven particle acceleration [3], and nuclear physics [4]. The development of CPA technology [5] and OPCPA technology [6] has enabled the construction of Petawatt laser systems worldwide, such as the HERCULES facility in the USA [7], the PETAL facility in France [8], 4 PW Laser in South Korea [9], SG-II facility [10], and SULF-10 PW laser [11] in China. The corresponding focused peak intensity of such femtosecond lasers has reached 10^{22}-10^{23} W/cm^2 [12]. In the development of a USUI laser, a high-energy pump source is one of the crucial factors. To illustrate, let's consider a typical 10 PW laser pulse with an energy of 300 J and a duration of 30 fs. The energy of the laser pulse before compression should exceed 500 J, taking into account energy loss in the compressor. Consequently, the total pump energy is up to 1 kJ calculated at 50% conversion efficiency. However, it is widely known that the high energy output and high repetition rate requirements pose a contradiction, which significantly constraining the average power of solid-state lasers, particularly those utilizing rod amplifiers. Waste heat can adversely affect beam quality by causing thermal distortions, thermal lens and some other thermal effects. Consequently, the implementation of efficient thermal management techniques is essential to dissipate the generated heat and maintain the desired beam quality.

Diode-pumped solid-state laser (DPSSL) systems are extensively used as pump sources for PW laser systems, primarily due to their low heat deposition and high optical-to-optical efficiency [13-16]. However, these systems are complex and expensive, which makes manual operation challenging and necessitates a significant investment. For applications requiring lasers with high energy output but lower demands on repetition rate, a cost-effective alternative is water-cooled rod-based lasers pumped by flashlamps [17-19]. Among the gain media commonly used in high-energy lasers, Nd-doped gain mediums are advantageous for generating high-energy pulses due to its relatively large emission cross section, high energy storage capacity, and a simple energy level structure. Commercial solutions have also been developed for pumping, such as the ATLAS 100J/1ppm by Thales and the 16J/5Hz pump laser system by Amplitude.

Based on the analysis above, Nd-doped rod amplifiers pumped by flash lamps are suitable for developing high-energy nanosecond-pumped lasers. However, rod amplifiers capable of achieving high-energy output cannot operate at high repetition rates due to their low heat dissipation ability. Thus, high energy and high repetition rates pose a constraint. In this study, taking the home-made pump units in SULF-10PW and our previous self-built pump lasers in SEL-100PW prototype as examples, the technical scheme of rep-rate pump laser based on rod amplifiers were investigated. Besides, the spatiotemporal evolution, thermal effects and frequency-doubled progress

were thoroughly studied. This study holds immense significance for the research of 10 PW USUI lasers and has crucial applications in other fields of high-energy lasers, such as advanced material processing [20] and laser shock peening [21].

2. Simulation and Experimental results

Firstly, the pump energy of the flash lamps can be determined based on the output energy of the power supply. Subsequently, the stored energy and thermal load can be calculated using the computed pump efficiency. Additionally, the absorption efficiency of the pump cavity and the distribution of energy storage in the gain rod can be calculated using the Monte Carlo ray tracing method. Based on the calculated energy storage above, the gain of the amplifier can be calculated using the Frantz-Nodvik equation. However, the conventional Frantz-Nodvik equation is typically used to calculate the overall gain, and adjustments are necessary to account for spatial and temporal variations of the laser pulse. Once the desired gain performance is established, thermal analysis can be conducted to determine the appropriate repetition rate of the amplifier.

2.1 Gain performance

Considering the cost of engineering construction, large-diameter rod gain media are typically pumped by flash lamps. The emitted flash spectrum covers the absorption peak of the gain medium, although not all spectral components emitted are absorbed. Hence, it is essential to calculate the absorption efficiency of the gain medium by analyzing its absorption spectrum and the radiation spectrum of the flash lamps. The calculations revealed that the spectrum overlap rate was around 15% based on self-established code. Monte Carlo ray tracing model can be employed to determine the absorption efficiency of pump light for various pump structures. In this model, the flash lamp was modeled as a Lambertian radiator. Additionally, there exists a plasma region in the center of the lamp, which absorbs most of the light as the pump light passes through this area. The reflective property was set as ABG scattering reflector. The absorption efficiency, as calculated by the Monte Carlo ray tracing model, was around 14%. Consequently, the overall pump efficiency was estimated to be approximately 2%, aligning with the typical expectations.

The stored energy can be calculated with pump efficiency, the gain performance of various amplifiers can be evaluated using the well-known Frantz-Nodvik equation. Figure 1 illustrates the comparison between theoretical and experimental results in the pump unit of SULF-10 PW. The first-stage amplifier in this pump unit consisted of two Nd: glass rods with diameters of 25 mm and a length of 280 mm, while the second-stage amplifier included two Nd: glass rods with diameters of 50 mm and a length of 280 mm. All Nd: glass rods were N31 phosphate glasses with a doping concentration of 0.5%. The arc length of the pump flash lamps was 250mm. As depicted in Figure 1, the experimental results closely matched the theoretical results. Also, the output energy increased linearly with the rise of the stored energy, indicating the absence of gain saturation because the stored energy is directly proportional to the pumped energy. This suggests the potential to increase the energy of this pump unit.

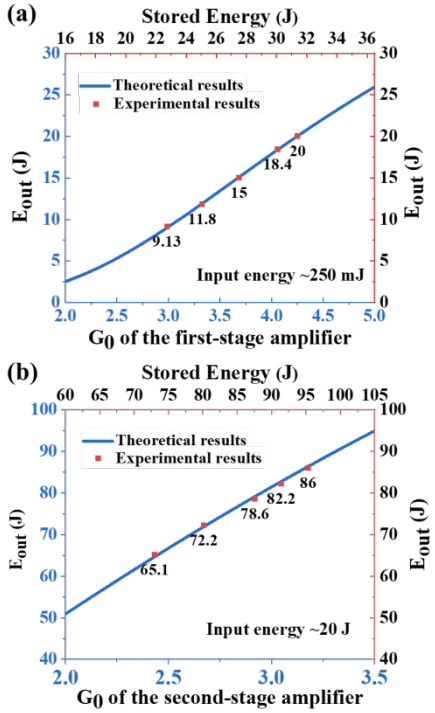

Fig.1. The theoretical (blue) and experimental results (red) of the output energy of (a) the first-stage amplifier and (b) the second-stage amplifier against gain factor G_0 in two stage amplifiers in the pump unit of SULF-10 PW.

However, rod amplifiers have a drawback in that the stored energy in the cross-section of the rod is rarely uniform, especially for large-diameter rods. This is attributed to the fact that the pump light is primarily absorbed at the edge of the rod, resulting in weaker pump light as it approaches the center of the rod. This non-uniformity in pumping can be improved by changing the structure of the reflective cavity, altering the doping concentration, or increasing the pump energy.

Specific experiments were conducted in the pump unit of SULF-10 PW. Firstly, the home-made seed sources were carefully designed to produce a super-Gaussian distribution beam profile, as shown in Figure 2(a). Subsequently, this super-Gaussian beam underwent double-pass amplification, comprising two amplification modules with 25 mm diameter Nd: glass rods. In the previous design, gold-plated involute reflectors were utilized, and the findings indicated that the stored energy in the rod's center exceeded that at the edges due to the higher beam intensity at the center. In order to achieve a more uniform beam profile, the gold-plated involute reflectors were substituted with elliptical reflectors fabricated from a diffuse reflection material. Regrettably, as shown in Figure 2(c), the amplified beam profile initially

displayed a "hollow-shaped" intensity distribution due to the relatively high doping concentration (1.2%). Subsequently, by reducing the doping concentration to 0.5%, the beam profile achieved greater uniformity, as depicted in Figure 2(b).

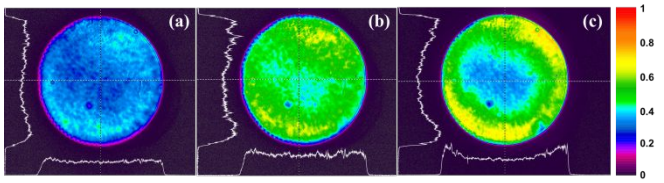

Fig.2. The beam profile of (a) super-Gaussian seed, (b) seed amplified by 25 mm diameter Nd: glass with 0.5% doping rate and (c) seed amplified by 25 mm diameter Nd: glass with 1.2% doping rate

However, achieving gain uniformity becomes more challenging when using rods with larger diameters, such as 50 mm. Figure 3(a) displays the final output beam profile after amplification by a 50 mm diameter Nd: glass rod with a 0.5% doping rate. The results indicate that the gain at the edge of the Nd: glass rod is higher than at the center. Additionally, the distribution of stored energy can be calculated using Monte Carlo ray tracing. This calculated distribution of stored energy is depicted in Figure 3(b) and aligns with the measured results. Furthermore, achieving a uniform beam profile can be accomplished by adjusting the injected beam profile or increasing the pump energy. The latter approach is more straightforward to implement and comprehend physically, as sufficient pump energy can maximize the excitation of particles, leading to a uniform distribution of stored energy. However, this approach may lead to inefficient use of pump energy and potential damage to subsequent optical elements due to the high energy flow density and narrowing pulse width associated with increased gain. An alternative method involves modifying the injected beam profile, which in turn places requirements on the output beam profile of the preceding stage. Specifically, in instances where there is higher stored energy at the edge, an injected Gaussian beam can be converted into a top-hat beam. Experimental validation has confirmed the effectiveness of this method.

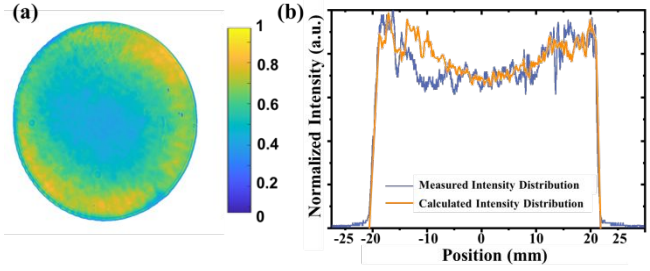

Fig.3. (a) The final output beam profile after amplified by 50 mm diameter Nd: glass with 0.5% doping rate; (b) The calculated and measured stored energy distribution across the beam cross section.

Based on the preceding analysis and taking into account pump uniformity, it is recommended to use rod gain mediums with diameter smaller than 50 mm. Rod gain medium with larger diameter can achieve higher output energy but may result in an uneven beam profile. While a multi-pass amplification scheme can eliminate beam profile inhomogeneity, it also increases the risk of potential damage to the optical components due to higher output energy.

2.2 Thermal management

Thermal management is also a crucial aspect in the design of a high-energy pump laser. Finite element analysis (FEA) is employed to evaluate the temperature distribution of the gain rods, and from the obtained data in FEA, the calculation of thermal birefringence becomes possible. Firstly, the temperature distribution can be determined through transient analysis or steady-state analysis, depending on the specific situation. The transient method was to calculate the temperature distribution incrementally combined with the Metro-Kalo ray-tracing method. Typically, the low repetition rate of high-energy rod amplifier ensures the accuracy of this method. Eventually, the temperature stabilizes at a quasi-steady state, allowing for the analysis of thermal effects based on the transient data when the pulse reaches. An alternative approach to deducing the thermal load is to directly analyze the steady state using the calculated stored energy and the quantum efficiency of the gain medium. Both methods are effective for analyzing thermal effects in most situations, with the transient method being more precise only in cases where the stored energy distribution in the gain medium is highly non-uniform. Taking the pump unit of SULF-10 PW as an example, Figure 4 illustrates the comparison of these two methods based on the 50 mm Nd: glass rod in SULF-10PW, where the pump distribution is relatively uniform. The results indicate that the final calculated state was nearly identical for both the maximum temperature of the gain medium. Through a basic analysis of the temperature distribution and thermal stress, the maximum repetition rate can be determined. We deduced, based on theoretical analysis and engineering experience, that the maximum safe average power for nanosecond solid-state amplifiers using flashlamp-pumped rod amplification is 200 W. In our constructed nanosecond flashlamp-pumped lasers with rod amplifiers, the high average power was measured at 60 W (1.2 J, 50 Hz) and 200 W (20 J, 10 Hz), both utilizing Nd: YAG rods. The 60 W laser employed two amplification modules with 8 mm diameter Nd: YAG rods, while the 200 W laser consisted of three amplification stages, incorporating Nd: YAG rods with diameters of 8 mm, 12 mm, and 21 mm. Further enlarging the diameter of the rod to will decrease the heat dissipation ability. Moreover, the temperature of the laser amplifier's shell noticeably increased when the output power reached 200 W and this pump laser operated at less than 200 W for safety reasons. Additionally, operating at

50 Hz would evidently reduce the flash lamps' lifetime. Therefore, based on engineering practice, 200 W appears to be the maximum average power for flashlamp-pumped high-energy rod amplifiers. Innovative thermal management approaches are necessary to assess the average power of solid-state lasers.

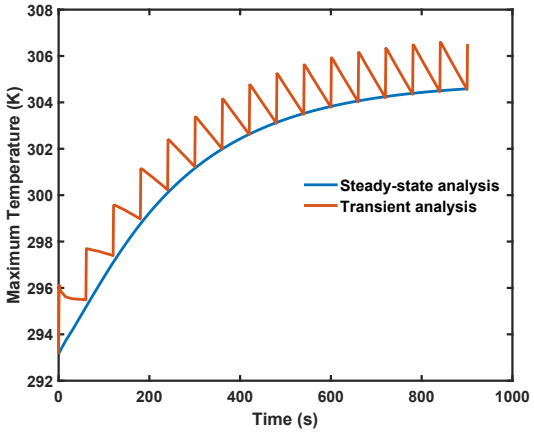

Fig.4. The comparison of the calculated results based on transient analysis (blue line) and steady-state analysis (orange line) method

In addition to analyzing temperature distribution and thermal stress distribution, it is important to consider other thermal effects, such as thermal birefringence and thermal distortion. A custom code was developed to calculate the thermal birefringence and thermal distortion. The comparison between theoretical and experimental results, as shown in Figure 5, revealed a strong agreement between the calculated and experimental outcomes.

To illustrate the validity of the calculated results, rods with diameters of 25mm and 50mm were selected. As previously mentioned, these two different types of Nd: glass rods were used in the 100J pump unit of SULF-10 PW. The gain data was presented previously. Figure 5 demonstrates the alignment of the measured thermal depolarization patterns with the simulated results. These thermal depolarization patterns were measured through TFPs without any method of compensating thermal depolarization. To mitigate the adverse impact of thermal birefringence, each stage of the amplifier consisted of two amplification modules with a polarization rotator positioned between them.

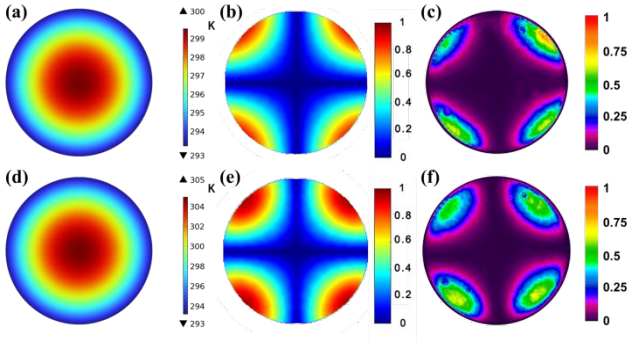

Fig.5. The simulated (a) temperature distribution and (b) thermal depolarization of Nd: glass rods with a diameter of 25mm. The simulated (d) temperature distribution and (e) thermal depolarization of Nd: glass rods with a diameter of 50mm; The measured thermal depolarization of (c) Nd: glass rods with a diameter of 25mm and (f) Nd: glass rods with a diameter of 50mm

Thermal distortion is a crucial factor to consider in pumping OPCPA due to the impact of wavefront distortion on the OPA process. The wavefront distortion primarily arises from three effects: thermal expansion, thermal-stress-induced index variation, and thermal-optical effects. Through FEA analysis, temperature distribution, stress distribution, and displacement data can be determined. Subsequently, the initial data were input into a self-developed code to compute the thermal distortion. As the thermal wavefront of the rod gain medium at low repetition rates is often too subtle for detection by a wavefront sensor, specific experiments were conducted at 50 Hz. Nd: YAG was selected as the gain medium due to its higher thermal transformation coefficient. In fact, for flash-pumped rod amplifier operating at high repetition rate, the heat generated by flash lamps was much larger than rod gain medium itself. However, considering the cost, flash lamps are much cheaper than LD laser. Figure 6 shows the measured and calculated wavefront distortion of Nd: YAG rod under different pump voltages. Although the wavefront distortion distribution was ununiform, the total value and the distribution trend was consistent. The uneven distribution of the wavefront was attributed to non-uniform heat dissipation. Additionally, wavefront distortion varied during each pulse, limiting the repetition rate of the flash-pumped rod amplifier. While one solution to this issue is to use an SBS mirror to compensate for wavefront distortion, it may cause reflective loss. Therefore, the rod-based amplifier should operate at a low repetition rate when wavefront distortion needs to be minimized.

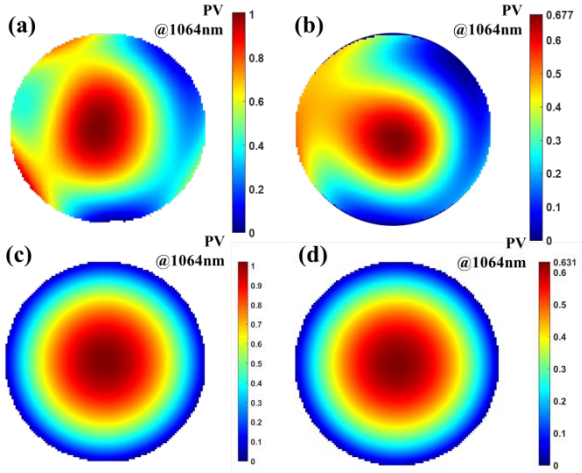

Fig.6. The measured wavefront distribution of Nd: YAG rod under 800V(a) and 700V (b) pump voltage operating at 50 Hz. The simulated wavefront distribution of Nd: YAG rod under 800V(c) and 700V (d) pump voltage operating at 50 Hz.

2.3 Temporal evolution during the amplification process

During the amplification process, the laser beam may experience temporal distortions due to gain saturation,

leading to a narrowing of the pulse width. Reduced pulse width means increased peak intensity that can potentially harm laser components. Thus, mitigating damage caused by pulse width narrowing is crucial. The full width at half maximum (FWHM) of the laser pulse is a widely used parameter for evaluating pulse width. By solving the modified Frantz-Nodvik equation, the evolution of pulse width can be simulated with a specific gain factor and appropriate size of the gain medium. Figure 7 illustrates the calculated evolution of pulse shape following the first-stage and second-stage amplification in a 100 J pump unit in SULF-10 PW. As shown in Figure 7, the pulse shape remains unchanged while the pulse width decreases from 17 ns in the seed laser to 15.4 ns during the amplification process, which is deemed acceptable for preventing optical damage. The measured pulse width of the final amplified pulse, as depicted in Figure 7, is 15.6 ns, closely aligning with the theoretical results.

A further requirement on laser pulse shape was temporal uniformity, namely, a square-wave pulse. The amplification of the leading edge of the pulse is higher than the trailing edge, which is a common phenomenon in laser amplifiers, and rod amplifiers exhibit this behavior as well. To achieve a square pulse, a triangular pulse with lower intensity at the leading edge is required. This required triangular pulse can be derived from the final output square-wave signal. Figure 8 demonstrates the evolution of pulse shape in the SEL-100PW pump prototype. As shown in Figure 8, the leading edge of the laser pulse has larger gain than the trailing edge. Thus, the pulse shape gradually becomes flatter and eventually becomes a nearly square-wave signal, which has a higher doubled frequency efficiency (up to 70%). For nanosecond high energy laser pulses, the properties of double frequency light inherit the characteristics of fundamental frequency light, such as the pulse shape and intensity distribution. Therefore, there is no need to worry about drastic changes in the temporal shape of the double-frequency light.

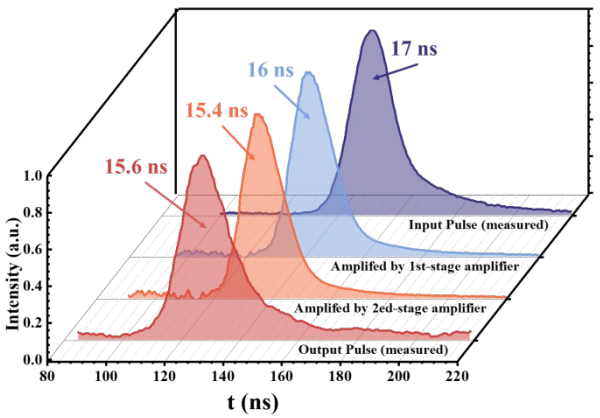

Fig.7. The evolution of the shape of the pulse through the amplification process in 100J pump unit of SULF-10PW. The measured input pulse (dark blue line), the calculated pulse shape after amplified by the first-stage amplifier (baby blue line), the calculated pulse shape after amplified by the second-stage amplifier (orange line) and the measured output pulse (red line)

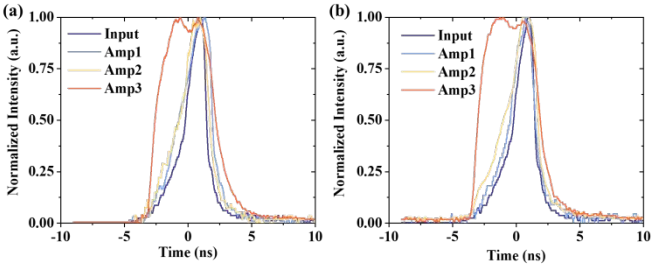

Fig.8. The evolution of the shape of the pulse through the amplification process in 25J pump unit of SEL-100PW prototype. (a) the calculated pulse shape evolution; (b) the measured pulse shape evolution;

3. Conclusion

In conclusion, a comprehensive multiphysics analysis of liquid-cooled flashlamp-pumped Nd-doped rods in high-energy nanosecond laser amplifiers was presented. The analysis encompassed gain performance, thermal effects and spatiotemporal evolution of laser pulses. Each aspect involved theoretical simulations and specific experiments, with results from both methods proving consistent. These analyses helped define certain performance limits of flash pump rod amplifiers. From an engineering standpoint, it is advised to maintain the average power of nanosecond pump lasers with flashlamp-pumped rod amplifiers below 200W. Furthermore, ensuring controllable wavefront distortion is crucial for pumping OPCPA, which, in turn, restricts the repetition rate of liquid-side cooling rod amplifiers. Despite inherent drawbacks associated with the rod-shaped configuration, flashlamp-pumped rod amplifiers are cost-effective, stable, and suitable for various high-energy nanosecond laser applications.

Funding. National Natural Science Foundation of China (11127901 and 62075227), National Major Scientific Research Instrument Development Project (22227901), National Key R&D Program of China (2019YFF01014401), Shanghai Municipal Science and Technology Major Project (2017SHZDZX02), the Shanghai Rising-Star Program (No. 21QA1410200), and the Youth Innovation Promotion Association CAS (No. 2020248). Innovation Funding Project of National Commercial Aircraft Manufacturing Engineering Technology Research Center (COMAC-SFGS-2021-603).

Disclosures. The authors declare no conflicts of interest.

References

1. S. G. Garanin, S. V. Garnov, A. M. Sergeev, and E. A. Khazanov, "Powerful Lasers for High Energy Density Physics," Herald of the Russian Academy of Sciences **91**, 250-260 (2021).
2. Y. Izawa, N. Miyanaga, J. Kawanaka, and K. Yamakawa, "High Power Lasers and Their New Applications," J. Opt. Soc. Korea **12**, 178-185 (2008).

3. P. A. Norreys, "Laser-driven particle acceleration," Nature Photonics **3**, 423-425 (2009).
4. R. Neugart, "Lasers in nuclear physics --A review," European Physical Journal A **15**, 35-39 (2002).
5. D. Strickland and G. Mourou, "Compression of amplified chirped optical pulses," Optics Communications **56**, 219-221 (1985).
6. A. Dubietis, G. Jonušauskas, and A. Piskarskas, "Powerful femtosecond pulse generation by chirped and stretched pulse parametric amplification in BBO crystal," Optics Communications **88**, 437-440 (1992).
7. V. Yanovsky, V. Chvykov, G. Kalinchenko, P. Rousseau, T. Planchon, T. Matsuoka, A. Maksimchuk, J. Nees, G. Cheriaux, G. Mourou, and K. Krushelnick, "Ultra-high intensity- 300-TW laser at 0.1 Hz repetition rate," Optics Express **16**, 2109-2114 (2008).
8. N. Blanchot, G. Béhar, J. C. Chapuis, C. Chappuis, S. Chardavoine, J. F. Charrier, H. Coïc, C. Damiens-Dupont, J. Duthu, P. Garcia, J. P. Goossens, F. Granet, C. Grosset-Grange, P. Guerin, B. Hebrard, L. Hilsz, L. Lamaignere, T. Lacombe, E. Lavastre, T. Longhi, J. Luce, F. Macias, M. Mangeant, E. Mazataud, B. Minou, T. Morgaint, S. Noailles, J. Neauport, P. Patelli, E. Perrot-Minnot, C. Present, B. Remy, C. Rouyer, N. Santacreu, M. Sozet, D. Valla, and F. Laniesse, "1.15 PW compressed beam demonstration using the PETAL facility," Opt. Express **25**, 16957-16970 (2017).
9. C. H. Nam, J. H. Sung, H. W. Lee, J. W. Youn, and S. K. Lee, "Performance of the 20 fs, 4 PW Ti:Sapphire Laser at CoReLS," in *Conference on Lasers and Electro-Optics*, OSA Technical Digest (online) (Optica Publishing Group, 2018), STu4O.3.
10. J. Zhu, X. Xie, Q. Yang, J. Kang, H. Zhu, A. Guo, P. Zhu, Q. Gao, Z. Liu, Q. Fan, D. Liu, X. Oyang, H. Wei, and X. Wang, "Introduction to SG-II 5 PW Laser Facility," in *Conference on Lasers and Electro-Optics*, OSA Technical Digest (2016) (Optica Publishing Group, 2016), SM1M.7.
11. W. Li, Z. Gan, L. Yu, C. Wang, Y. Liu, Z. Guo, L. Xu, M. Xu, Y. Hang, Y. Xu, J. Wang, P. Huang, H. Cao, B. Yao, X. Zhang, L. Chen, Y. Tang, S. Li, X. Liu, S. Li, M. He, D. Yin, X. Liang, Y. Leng, R. Li, and Z. Xu, "339J high-energy Ti:sapphire chirped-pulse amplifier for 10PW laser facility," Opt. Lett. **43**, 5681-5684 (2018).
12. Z. Li, Y. Leng, R. J. L. Li, and P. Reviews, "Further Development of the Short-Pulse Petawatt Laser: Trends, Technologies, and Bottlenecks," (2023).
13. P. Mason, S. Banerjee, K. Ertel, P. J. Phillips, M. De Vido, O. Chekhlov, M. Divoky, J. Pilar, J. Smith, T. Butcher, W. Shaikh, C. Hooker, C. Hernandez-Gomez, T. Mocek, C. Edwards, and J. Collier, "A 100J-level nanosecond pulsed DPSSL," in *Conference on Lasers and Electro-Optics*, OSA Technical Digest (2016) (Optica Publishing Group, 2016), STu3M.1.
14. S. Banerjee, P. Mason, J. Smith, J. Phillips, T. Butcher, S. Tomlinson, J. Suarez-Merchan, T. Zata, M. Hassan, I. Hollingham, A. Norton, D. Möller, H. Höppner, K. Ertel, M. De. Vido, B. Costello, A. Lintern, M. Tyldesley, C. Hernandez-Gomez, T. Toncian, U. Zastrau, E. Brambrink, C. Edwards, and J. Collier, "100J-level cryogenic gas cooled DPSSL for high energy density experiments at the European XFEL facility," in *Laser Congress 2018 (ASSL)*, OSA Technical Digest (Optica Publishing Group, 2018), AM2A.1.
15. S. Banerjee, P. D. Mason, K. Ertel, P. Jonathan Phillips, M. De Vido, O. Chekhlov, M. Divoky, J. Pilar, J. Smith, T. Butcher, A. Lintern, S. Tomlinson, W. Shaikh, C. Hooker, A. Lucianetti, C. Hernandez-Gomez, T. Mocek, C. Edwards, and J. L. Collier, "100J-level nanosecond pulsed diode pumped solid state laser," Opt. Lett. **41**, 2089-2092 (2016).
16. P. Mason, M. Divoký, K. Ertel, J. Pilař, T. Butcher, M. Hanuš, S. Banerjee, J. Phillips, J. Smith, M. De Vido, A. Lucianetti, C. Hernandez-Gomez, C. Edwards, T. Mocek, and J. Collier, "Kilowatt average power 100J-level diode pumped solid state laser," Optica **4**, 438-439 (2017).
17. A. K. Poteomkin, E. V. Katin, E. A. Khazanov, A. V. Kirsanov, G. A. Luchinin, A. N. Mal'shakov, M. A. Martyanov, A. Z. Matveev, O. V. Palashov, and A. A. Shaykin, "A compact 100J/100GW Pump Laser for Broadband Chirped Pulse Optical Parametric Amplifier," in *Conference on Lasers and Electro-Optics/Quantum Electronics and Laser Science and Photonic Applications Systems Technologies*, Technical Digest (CD) (Optica Publishing Group, 2005), CMA3.
18. A. K. Poteomkin, E. V. Katin, E. A. Khazanov, A. V. Kirsanov, G. A. Luchinin, A. N. Mal'shakov, M. A. Martyanov, A. Z. Matveev, O. V. Palashov, and A. A. Shaykin, "A 100 J 1 ns Nd:glass Laser for Optical Parametric Chirped Pulse Amplifiers Pumping," in *Advanced Solid-State Photonics*, Technical Digest (Optica Publishing Group, 2005), TuB42.
19. A. K. Poteomkin, E. V. Katin, E. A. Khazanov, A. V. Kirsanov, G. A. Luchinin, A. N. Mal'shakov, M. A. Martyanov, O. V. Palashov, and A. A. Shaykin, "Tabletop 300J 1ns Nd:glass Laser for Pumping of a Chirped Pulse Optical Parametric Amplifier," in *Advanced Solid-State Photonics*, OSA Technical Digest Series (CD) (Optica Publishing Group, 2007), WD5.
20. J. Natarajan, Y. Che-Hua, and K. Durairaj Raj, "Laser Surface Modification of Materials," in *Practical Applications of Laser Ablation*, Y. Dongfang, ed. (IntechOpen, Rijeka, 2020), p. Ch. 4.
21. S. Qutaba, M. Asmelash, K. Saptaji, and A. Azhari, "A review on peening processes and its effect on surfaces," The International Journal of Advanced Manufacturing Technology **120**, 4233-4270 (2022).